Ahmed NAIT OUSLIMANE[1], Hassane MOHELLEBI[1], Quang Anh PHAN[2]

Faculty of Electrical and Computer Engineering, Tizi-Ouzou University, Algeria (1),
Grenoble Electrical Engineering Laboratory (G2Elab), University of Grenoble, France (2)

An improved stress-dependent model for magnetomechanical effect simulation of Terfenol-D rods

Abstract. Terfenol-D is one of the smart materials widely used in the fabrication of magnetostriction based sensors and actuators due to its high material properties. However, using Terfenol-D in industrial applications rely on the ability of predicting its hysteresis by mathematical models. In this paper, we present an improved hysteresis model for reproducing hysteresis curves of Terfenol-D. Levenberg–Marquardt algorithm is used to estimate the optimal parameters of the improved model. The simulation and experimental results show the performances of the proposed model.

Streszczenie. Artykuł zajmuje się Terfenolem-D – dość powszechnie stosowanym materiałem magnetostrykcyjnym. Niestety dotychczas brakowało matematycznego modelu tego materiału uwzględniającego histerezę. Wykorzystano algorytm Levenberg–Marquardt do bardziej szczegółowego opisu parametrów Terfenolu. (Ulepszony model matematyczny opisujący efekt magnetostrykcyjny Terfenolu-D)

Keywords: Terfenol-D, Hysteresis, Levenberg-Marquardt algorithm, Finite element method.
Słowa kluczowe: efekt magnetostrykcyjny, Terfenol-D, histereza..

Introduction

Terfenol-D is a sort of the magnetostrictive materials widely used in the manufacturing of sensors and actuators due to its superior characteristics such as high force (up to 15kN), large strain (up to 2000ppm) and fast speed response (up to 100 kHz) [1, 2, 3]. Like any other ferromagnetic materials, Terfenol-D presents hysteresis, which makes its magnetomechanical behavior nonlinear [4]. This nonlinearity and hysteresis make it difficult to control. Modelling the hysteresis of Terfenol-D is more problematic than that of usual ferromagnetic materials. One complexity is that the hysteresis of Terfenol-D is a function of mechanical parameters like stress and strain [5, 6, 7]. In order to accurately model the magnetomechanical behaviour of Terfenol-D, models for magnetic materials must be modified.

A number of mathematical models have been developed to describe hysteresis of Terfenol-D, such as Preisach model [8], Prandtl–Ishlinskii model [9, 10], Jiles-Atherton model [11, 12], hyperbolic tangent model [13], and homogenized energy model …etc.

The Preisach model [14], was at first developed for ferromagnetic materials and is now frequently used to model magnetostrictive materials such Terfenol-D. The model developed for regular magnetic materials has only a single input parameter and a single output one. Considering that Terfenol-D has four parameters (magnetization, external magnetic field, strain, and stress), different choices for input and output are possible when using the Preisach model [15]. However, Preisach model is developed based on the first order reversal curves that are obtained under fixed conditions which are driving frequency and mechanical load. The Preisach model needs a large number of parameters to be identified, thus the model is not easily used in the case of the changing operating conditions [16].

The homogenized energy model [17] is established based on modeling the Helmholtz free energy of domain wall in ferromagnetic materials. In [18] the homogenized energy model is adopted to build up a magnetomechanical hysteresis model by assuming the physical variables to be functions of the mechanical load. The weighting functions similar to the Preisach model needs experimental data to be identified. One of the limitations of this approach is that a big experimental data is required for determination of the weighting function parameters.

The Jiles–Atherton (JA) model is an energy-based physical model for modelling hysteresis of ferromagnetic materials under zero stress and varying magnetic field. In [19], the JA model is modified to describe the magnetoelastic behavior of magnetic materials. Obviously the JA model parameters are related not only to the mechanical load stress, but also on the given bias of the magnetic field [20]. Consequently, this mathematical model is not appropriate to globally describe the magnetostrictive effect of materials. There is a possibility to use the JA model and the theory of magnetomechanical effect to describe the magnetomechanical behavior of Terfenol-D under various mechanical and magnetic conditions, but this is not much studied in the literature.

The arctangent model covers the physical properties of Terfenol-D in a very accurate way [7]. A drawback of this method is that the parameters of the hysteresis curves have to be calculated numerically. This leads on one hand to a slight increase of computation time and on the other hand to some complications with regard to the numerical solution of the problems.

In this paper, an improved magnetomechanical hysteresis model of Terfenol-D devices for precise and controlled applications is established based on an arctangent effective field model and the theory of magnetomechanical effects. The definition of effective magnetic field used here is different from that in previous works [1, 6, 7]. The effective magnetic field is not part of the model parameters and it is expressed in terms of magnetic flux density B instead of magnetization M, then the complexity of the model is significantly decreased. Levenberg–Marquardt algorithm is used to estimate the optimal parameters of the proposed model. The latter are considered in finite element analysis to conduct simulations of magnetostrictive behavior of Terfenol-D rods. Comparisons between the calculated and measured results show the accuracy of the proposed model.

Hysteresis model of Terfenol-D

In this section, we develop an improved hysteresis model for Terfenol-D rods, by extending the arctangent model. For magnetostrictive materials, there is an algebraic relation between magnetic field and magnetostriction phenomena. The following polynomial function relates magnetic flux density B to displacement:

$$(1) \qquad \varepsilon_{ij}^{m}(B, \sigma) = \gamma_0(\sigma).B^2 + \gamma_1(\sigma).B^4$$

where γ_0 and γ_1 are constants of mechanical load and ε_{ij}^m is the magnetostriction. By using this relation, magnetostriction control is achieved by controlling the magnetic flux density.

Magnetostriction ε_{ij}^m takes into account only the strain caused by magnetization. For total strain ε, the mechanical strain should be added.

The parameters γ_0 and γ_1 determine how the magnetostriction curve changes when the applied stress is changed. By considering a linear relationship between γ_i and σ, we obtain:

(2) $\quad \varepsilon_{ij}^m(B,\sigma) = (\beta_0(\sigma) + \sigma\,\beta_1(\sigma))\,B^2 + (\beta_2(\sigma) + \sigma\,\beta_3(\sigma))\,B^4$

The magnetostriction effect as a mechanical phenomenon can be correlated to the magnetic phenomena using the arctangent model in order to study the effect of stress on the magnetic behavior of Terfenol-D [21]. Based on both the thermodynamics and mechanical equilibriums, we describe the influence of stress on the magnetization with an additional term in the expression witch is the effective field.

For weak and moderate fields, the magnetic flux density can be described by an arctangent function, given by:

(3) $\quad F = c_1 . \arctan\left(\left(\frac{\alpha - 1}{c_1} \right) . \mu_0 . H_i(B,\varepsilon) \right) + \mu_0 . H_i(B,\varepsilon)$

With $c_1 = \dfrac{2 b_{sat}}{\pi}$, b_{sat} and α are flux density saturation, identified parameter respectively,

It was established that for a wide range of stress, the so-called effective field $H_i(B,\varepsilon)$ was just a product of two terms, function of stress $k(\sigma)$ and function of magnetic field density. The effect of the magnetostriction phenomenon due to the applied magnetic field on a terfenol-D rod can be explained in mechanical constitutive laws [22].

The magnetization at any stress level can be implicitly calculated as:

(4) $\quad H_i(B,\varepsilon) = H_i^0(B,\varepsilon) - k(\sigma)\,\dfrac{\partial \varepsilon_{kl}^m(B)}{\partial B_i}$

(5) $\quad H_i(B,\varepsilon) = H_i^0(B,\varepsilon) - H_i^c(B,\varepsilon)$

where ε_{kl}^m, $H_i^c(B,\varepsilon)$ and $H_i^0(B,\varepsilon)$ represent the magnetostriction tensor, the magnetic field induced by the effect of magnetostriction and the magnetic field at zero stress depending only on the magnetic flux density B respectively.

The parameters of the magnetostrictive model were found for each applied stress value by fitting the calculated curves to the measured curves by using Levenberg Marquardt Algorithm.

Parameter optimization method

Levenberg Marquardt algorithm (LMA) [23] is a Newton-type gradient iterative method, that locates a local minimum of an objective function defined as the sum of squares of difference between model estimated outputs and experimental data. Levenberg Marquardt method is just a switch rule between steepest descent and Gauss Newton method. When the solution is far from a local minimum, the algorithm behaves similar to steepest descent method with guaranteed convergence. Once the solution is close to the local minimum, it becomes the Gauss Newton method and shows fast convergence [24].

For the Terfenol-D rod, strain and magnetization are measured using an experimental setup at five different loads from 0 to 24 MPa. The parameters in equations (1), (3) and (4) are selected to minimize the sum of squares error function given by the equation (6):

(6) $\quad I(\theta) = \dfrac{1}{2} \sum_{i=1}^{n} (B_{\exp} - B_{comp})^2 = \dfrac{1}{2} \sum_{i=1}^{n} e^2$

Where $B_{\exp}$, B_{comp} and n are the experimental value of magnetic flux density data, the computed one using magnetic and magnetostrictive models and a number of measurement data point respectively. The number n should be chosen sufficiently large in respect with the computational performances and reaction to fast changes. e is the prediction error. After the definition of the objective function, this latter is minimized with respect to the θ vector $\theta = [\theta_1, \theta_2, \theta_3, \dots \theta_m]$, where m is number of the unknown parameters. The minimization is carried out, in such a way, that it alloys to get the best matching between model and experimental data.

The LM algorithm is described as following:

(7) $\quad \left[J(\theta^k)' J(\theta^k) + \lambda . diag\left(J(\theta^k)' J(\theta^k) \right) \right] \delta\theta^k = J(\theta^k)' . G$

(8) $\quad \theta^{k+1} = \theta^k + \delta\theta^k$

where G, J, λ and k are the gradient of the cost function, Jacobian matrix, damping parameter and the iteration number respectively.

The Jacobian matrix is a n x m matrix defined by:

(9) $\quad J(\theta) = \begin{bmatrix} \dfrac{\delta B(1,\theta)}{\delta\theta_1} & \dfrac{\delta B(1,\theta)}{\delta\theta_2} & \cdots & \dfrac{\delta B(1,\theta)}{\delta\theta_6} \\ \dfrac{\delta B(2,\theta)}{\delta\theta_1} & \dfrac{\delta B(2,\theta)}{\delta\theta_2} & \cdots & \dfrac{\delta B(2,\theta)}{\delta\theta_6} \\ \vdots & \vdots & \cdots & \vdots \\ \dfrac{\delta B(n,\theta)}{\delta\theta_1} & \dfrac{\delta B(n,\theta)}{\delta\theta_2} & \cdots & \dfrac{\delta B(n,\theta)}{\delta\theta_6} \end{bmatrix}$

As shown in (7) when λ is large, the LMA tends towards the steepest descent method. And when λ has a small value the LMA approaches the Newton method. In case of intermediate λ, the LMA will moderate between the steepest and the Newton method. During the optimization process, the LMA is used to adapt the values of λ. If the solution is successful $I(\theta^k + \delta\theta^k) < I(\theta^k)$, is decreased to exploit more the information contained inside $\left[J(\theta^k)' J(\theta^k) + \lambda . diag\left(J(\theta^k)' J(\theta^k) \right) \right]$, if the iteration happens to result in a worse approximation $I(\theta^k + \delta\theta^k) > I(\theta^k)$, λ is increased in order to pursue closely the gradient.

(10) $\quad \lambda^{k+1} = \begin{cases} \lambda^k / r & I(\theta^k + \delta\theta^k) < I(\theta^k) \\ \lambda^k . r & I(\theta^k + \delta\theta^k) > I(\theta^k) \end{cases}$

where r is the factor for increasing or decreasing λ.

The procedure of parameter identification process with LMA is given as follows:

Step 1: the iteration number kk, initial parameters λ_1 and θ_1 are defined.

Step 2: θ^k used to calculate $B_{comp}(k,\theta^k)$ and $I(\theta)$ by equations

(1), (3), (4) and (6)

Step 3: calculate $J(\theta)$ by equation (9)

Step 4: calculate $\delta\theta^k$ by equation (7)

Step 5: $\theta^{k+1} = \theta^k + \delta\theta^k$ used to compute $B_{comp}(k, \theta^k)$ and $I(\theta^k)$

    by equations (1),(3), (4) and (6).

    If $I(\theta^k + \delta\theta^k) < I(\theta^k)$ then $\lambda^{k+1} = \lambda^k / r$ and

$\theta^{k+1} = \theta^k + \delta\theta^k$ otherwise $\lambda^{k+1} = \lambda^k . r$ and $\theta^{k+1} = \theta^k$

Step 6: if $k > kk$ LMA terminates and records θ^{k+1}, otherwise $k = k+1$ go to Step3.

In Fig. 1, the dependence of the total error (e) on the number of iterations is shown. It can be seen that the error quickly decreases and the search algorithm allows us to achieve the optimal set of parameters with minimum computational effort.
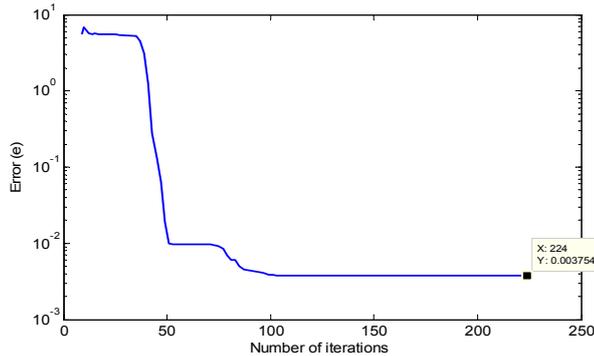
Fig.1: Total error depending on the number of iterations

The parameters, in equation (1) (3) and (4), are determined by Levenberg-Marquardt Method. The hysteresis magnetic curves at different load up to 24 MPa were compared to experimental data (fig. 2) [25], a good fit is obtained and it is seen that the magnetization continuously moves to higher fields with increasing stress. The obtained coefficients are listed in Table 1.

In the improved model, we use the difference between the magnetic field value $H_i(B, \varepsilon)$ at $\sigma = \sigma_{ref}$ and a value given at compressive stress load. The resulting field is used to be considered as an additional field and thus the effective field is given by:

(11) $H_i(B, \varepsilon) = \Delta H(B, \varepsilon) + H_i^0(B, \varepsilon) - H_i^c(B, \varepsilon)$

With

(12) $\Delta H_i(B, \varepsilon) = H_{\sigma_{ref}}(B, \varepsilon) - H_\sigma(B, \varepsilon)$

Table 1: identified model parameters

Parameters	Unit	values
β_0	$\left(\dfrac{m}{A}\right)^2$	$4.496 \cdot 10^{-2}$
β_1	$\left(\dfrac{m}{A}\right)^2 Pa^{-1}$	$1.0007 \cdot 10^{-10}$
β_2	$\left(\dfrac{m}{A}\right)^4$	$3.648 \cdot 10^{-3}$
β_3	$\left(\dfrac{m}{A}\right)^4 Pa^{-1}$	$7.7391 \cdot 10^{-11}$
α	1	$1.73588 \cdot 10^{-11}$
k	1	$1.412 \cdot 10^{+7}$

It is important to note that we can choose the identified parameters for each value of applied compressive stress

given by the table 1 as initial values to identify magnetic hysteresis loops at another applied stress. In this case, the size of the magnetic flux density vector and the magnetic field one must be the same. The results obtained from running LM algorithm to identify the optimal parameters of the improved model are listed in table 1.
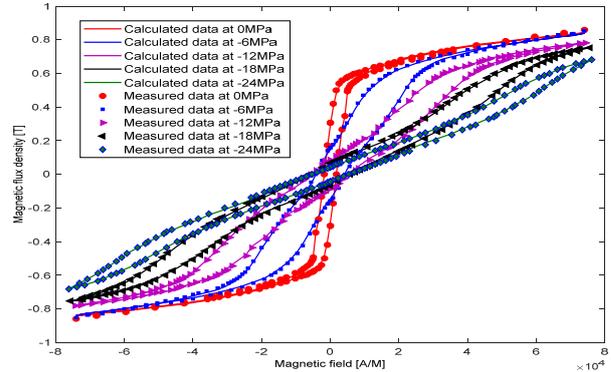
Fig.2. Hysteresis curves for different compressive stress values.

Magnetomechanical finite element formulation

Nowdays, an accurate modelling of non-linear magnetostrictive materials such as Terfenol-D is greatly needed. In this context, the optimal parameters, obtained from LMA, are used as numerical input to the simulation of the Terfenol-D rods behavior by means of a finite element code implemented using Matlab.

The partial differential equation of the magnetic problem, can be written as:

(13) $\dfrac{\partial}{\partial x}\left(\dfrac{1}{\mu_0}\dfrac{\partial A_z}{\partial x}\right) + \dfrac{\partial}{\partial y}\left(\dfrac{1}{\mu_0}\dfrac{\partial A_z}{\partial y}\right) = -\vec{J}_{sz} - \left(\dfrac{\partial M_y}{\partial x} - \dfrac{\partial M_x}{\partial y}\right)$

where μ_0 is the magnetic vacuum permeability, A_z the magnetic potential component vector and $\vec{J}_{sz}$ the current source density. The magnetization components M_x and M_y are a function of mechanical stress when the magnetostrictive property is included in the model.

The mechanical deformation of the rod, can be expressed as:

(14) $\sum_{j=1}^{n}\dfrac{\partial\sigma_{ij}}{\partial x_j} + f_i^v = \rho\dfrac{\partial^2 U_i}{\partial t^2}$ $i = 1 \ldots n$

were f_i^v represents the body forces, U_i is the mechanical displacement, ρ is the volume density, x_j is the nodal coordinate at node (i) and n the stress tensor order.

Many authors considered the equation (14) when solving the coupling magnetomechanical problem between magnetic field and mechanical deformation. In the most cases, the mechanical deformation equation is simplified to its one dimensional variation form. Consequently, only a one component of the strain has been usually considered in several studies [26, 27] but there is also a method based on definition of an equivalent stress of multi axial magneto-mechanical stress. The equivalent stress is deduced from one dimensional experimental data. In the current study, the strain ε and the stress σ are considered tensors quantities by defining two directions of deformations along x and y Cartesian coordinates.

The finite element formulation of the magnetomechanical problem using the principle of

orthogonality between the residual function R_i and a weighted function α_i, is given as follows:

$$(15) \qquad \int_\Omega R_i . \alpha_i . d\Omega = 0$$

With

$$(16) \qquad R_i = \sum_{j=1}^{n} \frac{\partial \sigma_{ij}}{\partial x_j} + f_i^{\,\nu} - \rho \frac{\partial^2 U_i}{\partial t^2}$$

By replacing R_i in equation (15), we obtain the following finite element integral formulation:

$$(17) \qquad \int_\Omega \left(\sum_{i,j}^{n} \frac{\partial \sigma_{ij}}{\partial x_j} + f_i^{\,\nu} - \rho \frac{\partial^2 U_i}{\partial t^2} \right) . \alpha_i . d\Omega = 0$$

In the case of elastic deformation, the stress tensor σ_{ij} behavior depends on the strain components ε_{ij}, which is given by:

$$(18) \qquad \begin{pmatrix} \sigma_{xx} \\ \sigma_{yy} \\ \sigma_{xy} \end{pmatrix} = \frac{E}{1-\nu^2} \begin{pmatrix} 1 & \nu & 0 \\ \nu & 1 & 0 \\ 0 & 0 & \frac{1-\nu}{2} \end{pmatrix} \begin{pmatrix} \varepsilon_{xx} \\ \varepsilon_{yy} \\ \varepsilon_{xy} \end{pmatrix}$$

where E is the Young modulus and ν is Poisson's ratio. The Terfenol-D rod, is assimilated to a plate of infinite dimension that deforms in bending only. In our case, we are handling the following 2D magnetomechanical equations:

$$(19) \quad \frac{E}{1-\nu^2} \frac{\partial^2 u_x}{\partial x^2} + \frac{\nu E}{1-\nu^2} \frac{\partial^2 u_y}{\partial x \partial y} + \frac{E}{4(1+\nu)} \frac{\partial^2 u_x}{\partial y^2} +$$

$$\frac{E}{4(1+\nu)} \frac{\partial^2 u_y}{\partial y \partial x} + f_x = \rho \frac{\partial^2 u_x}{\partial t^2}$$

$$(20) \quad \frac{E}{1-\nu^2} \frac{\partial^2 u_y}{\partial y^2} + \frac{\nu E}{1-\nu^2} \frac{\partial^2 u_x}{\partial x \partial y} + \frac{E}{4(1+\nu)} \frac{\partial^2 u_y}{\partial x^2} +$$

$$\frac{E}{4(1+\nu)} \frac{\partial^2 u_x}{\partial y \partial x} + f_y = \rho \frac{\partial^2 u_y}{\partial t^2}$$

Discretization and assembly of the local stiffness matrix and force vector source of each element constituting the plate lead to the following algebraic systems:

$$(21) \qquad [S][A] = [K] + [G]$$

where [S], [K], [G] and [A] are electromagnetic stiffness matrix, excitation current density vector, magnetic source field vector and magnetic potential vector, respectively.
Where,

$$S_{ij} = \iint_\Omega \left[\frac{\partial \{N_i\}}{\partial x} . \frac{\partial \{N_j\}^T}{\partial x} + \frac{\partial \{N_i\}}{\partial y} . \frac{\partial \{N_j\}^T}{\partial y} \right] d\Omega$$

$$K_i = \iint_\Omega \mu_0 \{N_i\} . J_{sz} d\Omega$$

$$G_i = \iint_\Omega \mu_0 \{N_i\} . \left(\frac{\partial M_y}{\partial x} - \frac{\partial M_x}{\partial y} \right) d\Omega$$

In fact, we may construct the system equations of magnetomechanical coupled phenomena given by an algebraic system expressed as follows:

$$(22) \qquad [M][U] = [F]$$

where [M], [F] and [U] are the mechanical stiffness matrix, body force vector and field displacement vector respectively.
With,

$$M = \begin{bmatrix} M_{11} & M_{12} \\ M_{21} & M_{22} \end{bmatrix}$$

$$M_{11} = \int_\Omega \left(\frac{E}{1-2\nu} \frac{\partial \alpha_i}{\partial x} \frac{\partial \alpha_j}{\partial x} + \frac{E}{4(1-\nu)} \frac{\partial \alpha_i}{\partial y} \frac{\partial \alpha_j}{\partial y} \right) dxdy$$

$$M_{21} = \int_\Omega \left(\frac{\nu E}{(1-\nu)(1-2\nu)} \frac{\partial \alpha_i}{\partial x} \frac{\partial \alpha_j}{\partial y} + \frac{E}{4(1-\nu)} \frac{\partial \alpha_i}{\partial y} \frac{\partial \alpha_j}{\partial x} \right) dxdy$$

$$M_{22} = \int_\Omega \left(\frac{E}{1-2\nu} \frac{\partial \alpha_i}{\partial y} \frac{\partial \alpha_j}{\partial y} + \frac{E}{4(1-\nu)} \frac{\partial \alpha_i}{\partial x} \frac{\partial \alpha_j}{\partial x} \right) dxdy$$

$$f_x = \int_\Omega \alpha_i f_x^{\,\upsilon} \, dxdy + \int_\Omega \alpha_i f_x^{\,m} \, dxdy + \int_\Omega \alpha_i f_x^{\,mst} \, dxdy$$

$$f_y = \int_\Omega \alpha_i f_y^{\,\upsilon} \, dxdy + \int_\Omega \alpha_i f_y^{\,m} \, dxdy + \int_\Omega \alpha_i f_y^{\,mst} \, dxdy$$
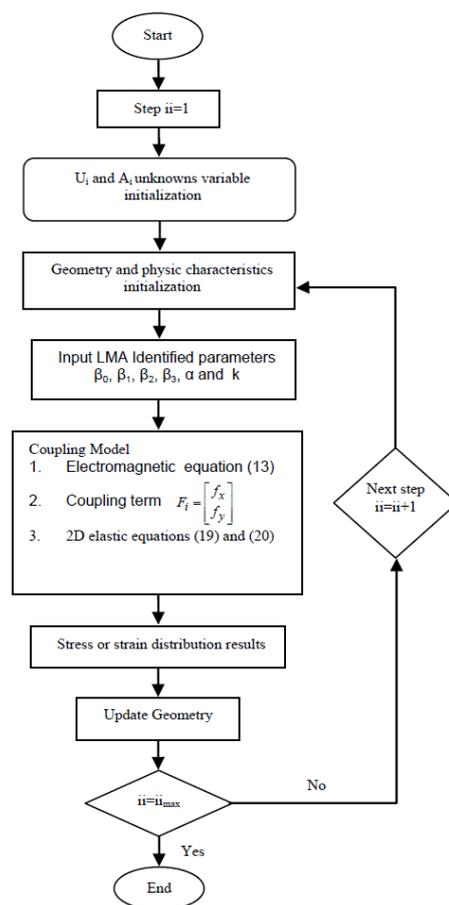
Fig.3: Flow chart of the FEM

The numerical solution of this problem is based on, finite element method, thanks to its superiority on solving nonlinear and complex geometry structures by integration of behavior laws. The flow chart of the FEM program is shown in fig. 3.

Application and results

The optimal parameters obtained from LMA can be injected in the finite element model to calculate the magnetostrictive strain values of Terfenol-D rods in response to applied magnetic field and compressive stress. Thus, we should calculate the magnetization, flux density and magnetic force under the same conditions to the problem configuration depicted in Fig. 4.
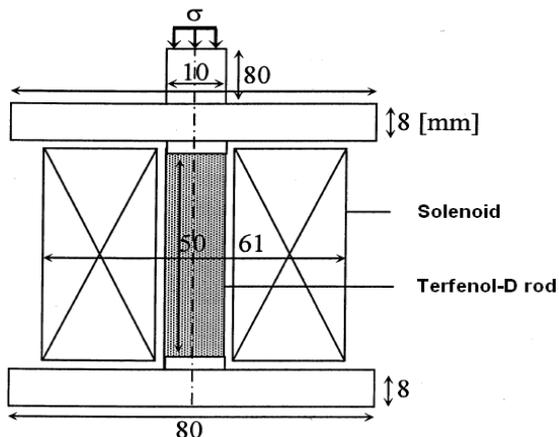
Fig.4. Schematic diagram of the magnetostrictive device

The device consists of a Terfenol-D rod under different loading and magnetic field values. We assume that the bottom end of the rod is fixed while the top one is free, and receive the mechanical load. The compressive stress is applied by a prestress bolt and a spring washer. The spring is quite soft to allow a constant compression for each stress state, when the rod changes size. The Terfenol-D rod is surrounded by a magnetic coil fed by a DC power supply unit which ensure the desired magnetic field. An optical encoder measures the displacement of the actuator. A pick-up coil measures the flux density B inside the Terfenol-D rod, and a load cell measures the force applied to the rod. Finally, an electronic circuit inside the power supply unit measures the current. The measurements made by the sensors are fed to a data acquisition card after being amplified by an electronic circuit. Using the test rig and a data collection method detailed, the major hysteresis curves of Terfenol-D are obtained at 5 different stress levels up to 24 MPa. At each stress level, the displacement produced by the actuator is also recorded.

(a)

(b)

(c)

(d)

(e)
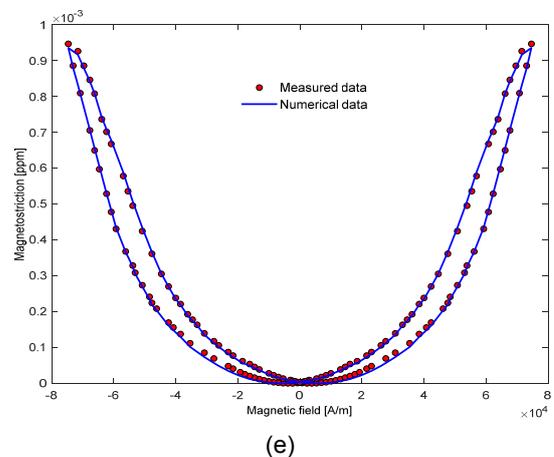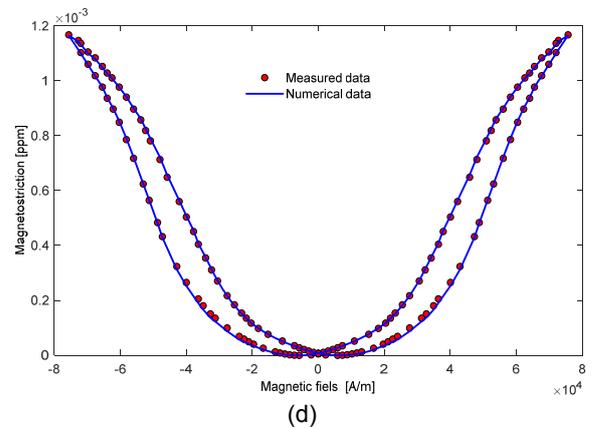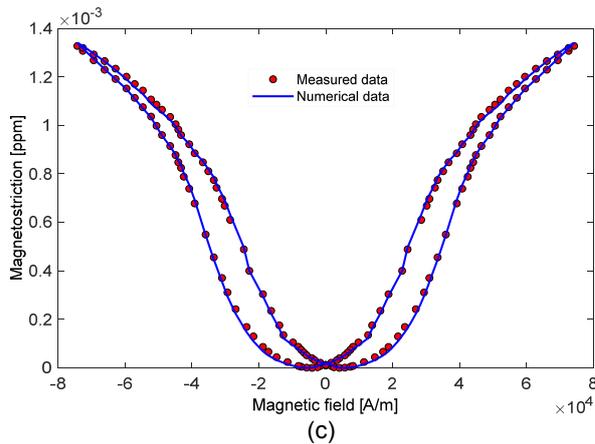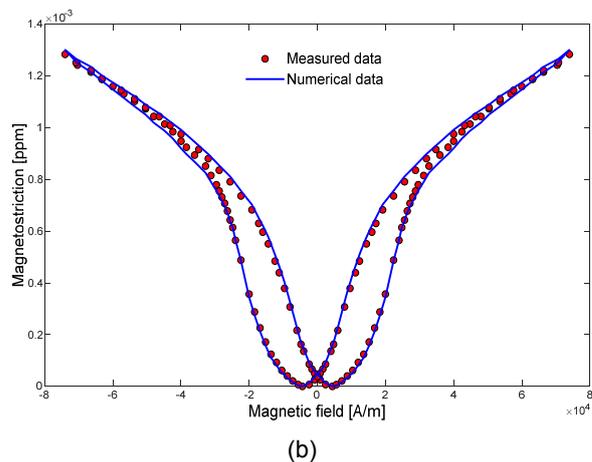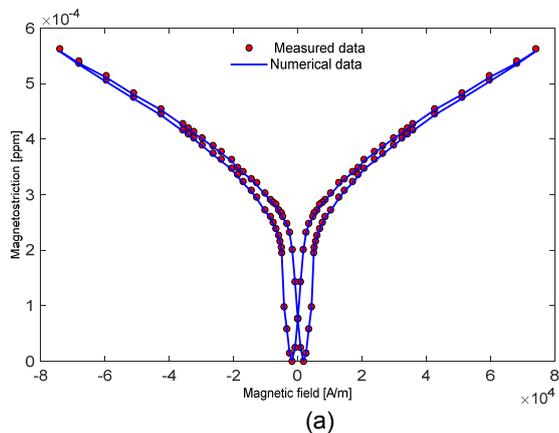
Fig.5. Magnetostriction curves versus magnetic field at different compressive stress values. (a) 0MPa. (b)-6MPa. (c)-12MPa. (d)-18MPa. (e)-24MPa

In Fig. 5, the curves of magnetostriction versus the magnetic field at different loads show the impact of the applied stresses on the resulted strain. The magnetostriction of the Terfenol-D rod is illustrated for applied stress varying from –6 MPa to –24 MPa [25, 28]. There is an excellent agreement between the experimental and numerically computed results for all applied stresses.

This analysis shows that the prediction of the improved model gives a good concordance with experimental data, specially by considering the linear relationship between γ_i and σ in the polynomial approximation of ε.

The finite element computation permits also to describe the operating process of the Terfenol-D devices and to develop models, which can be helpful for the design and optimization of new magnetostrictive structures.

Conclusion

An improved load dependent model for hysteresis in Terfenol-D rods is presented. The basis of the developed method is the arctangent effective field model. The model parameters were identified using Levenberg–Marquardt algorithm. In order to validate the improvements, a set of experimental hysteresis curves of Terfenol-D at different loads was used to identify the model parameters.

Comparison between the experimental and calculated results shows that the improved model can better describe magnetomechanical hysteresis behaviors of Terfenol-D rods under a varying compressive stress. The model parameters can be injected in a finite element analysis to predict the mechanical elongation of rods. Moreover, the formulation of the proposed model is quite simple, and has clear physical meaning which can ensure the simulation requirements, such as: speed, accuracy and good convergence. Finally, the improved model has a very strong engineering capabilities and can be considered in magnetostrictive devices designing and fabrication. Future studies will deal with more complex models, taking into account perturbing magnetic field, temperature and anisotropy effect in Terfenol-D rods.

Authors: *PhD student. Nait Ouslimane Ahmed, Faculty of Electrical and Computer Engineering, Mouloud Mammeri University of Tizi-Ouzou, BP 17RP 15000, Algeria, E-mail: naitouslimane.ahmed78@gmail.com; prof. dr. Hassane Mohellebi, Faculty of Electrical and Computer Engineering, Mouloud Mammeri University of Tizi-Ouzou, BP 17RP 15000, ALGERIA, E-mail :mohellebi@yahoo.fr , dr. Quang Anh PHAN, Grenoble Electrical Engineering Laboratory (G2Elab), Bâtiment GreEn-ER, 21 avenue des martyrs, CS 90624 38031 Grenoble CEDEX 1 FRANCE, E-mail: quang-anh.phan@g2elab.grenoble-inp.fr*

REFERENCES
[1] Zheng J., Cao S and Wang H., Modeling of Magnetomechanical Effect Behaviors in a Giant Magnetostrictive Device under Compressive Stress, *Sensors and Actuators* A.,143 (2008), 204-214
[2] Stachowiak D., The Influence of Magnetic Bias and Prestress on Magnetostriction Characteristics of a Giant Magnetostrictive Actuator, *Przegląd Elektrotechniczny*., 89 (2013), No. 4, 233-236
[3] Lopez J.D., Dante A., Cremonezi A.O., Ferreira E.C., Salles B.R and Gomes A.M., A Fiber-optic Current Sensor Based on FBG and Terfenol-D with Magnetic Flux Density Concentration, *In Proceedings of the IEEE Sensors.*, 20 (2019), 1-4
[4] Meng A., Zhu J., Kong M., and He H., Modeling of Terfenol-D Biased Minor Hysteresis Loops, *IEEE Trans. Magn.*, 49 (2013), No. 1, 552–557
[5] Jackiewicz D., Juś A., Szewczyk R and Bieńkowski A., Two Methods of Magnetoelastic Effect Utilization to Evaluate Mechanical Strain in the Truss Structures, *Przegląd Elektrotechniczny.*, 93 (2017) No. 7, 31-33

[6] Valadkhan S., Morris K and Shum A., A New Load-dependent Hysteresis Model for Magnetostrictive Materials, *Smart Mater. Struct.*, 19 (2010), 1-10
[7] Perevertov O., Influence of the Residual Stress on the Magnetization Process in Mild Steel, *J. Phys. D: Appl. Phys.*, 40 (2007) 949–954
[8] Kuczmann M., Measurement and Simulation of Vector Hysteresis, *Przegląd Elektrotechniczny (Electrical Review).*, 87 (2011), No. 3, 103-106
[9] Janaideh M.A., Naldi R, Marconi L., and Krejčí P., A Hybrid Model for the Play Hysteresis Operator, *Phys. B.,* 430 (2013), 95-98
[10] Minorowicz B., Nowak A and Stefanski F., Hysteresis Modelling in Electromechanical Transducer with Magnetic Shape Memory Alloy, *Przegląd Elektrotechniczny.*, 90 (2014), No. 11, 244-247
[11] Jiles D.C., Thoelke J.B., and Devine M.K., Numerical etermination of Hysteresis Parameters for the Modeling of Magnetic Properties Using the Theory of Ferromagnetic Hysteresis, *IEEE Trans. On Magn.*, 281 (1992), No. 1, 27-35
[12] Li, Y., Huang, W., Wang, B., and Weng, L.. High-Frequency Output Characteristics of Giant Magnetostrictive Transducer, *IEEE Trans. Magn.*, 55 (2019), No. 6, 1-5
[13] Talebian S., Hojjat Y., Ghodsi M., Karafi M.R., and Mirzamohammadi S., A Combined Preisach–Hyperbolic Tangent Model for Magnetic Hysteresis of Terfenol-D, Journal of Magnetism and Magnetic Materials., 396 (2015), 38-47
[14] Preisach F., *Z. Phys.,* 94 (1835), 277-302
[15] Jesenik M., Goričan V., Hamler A., Štumberger B., Trlep M., Numerical Scalar Hysteresis Model and its Precision, *Przegląd Elektrotechniczny.*, 87 (2011), No. 3, 85-88
[16] Adly A.A., Mayergoyz I.D., and Bergqvist A., Preisach Modeling of Magnetostrictive Hysteresis, *Journal of Applied Physics*, 69 (1991), 5777-5779
[17] Smith R.C., and Dapino M.J., A Homogenized Energy Model for the Direct Magnetomechanical Effect, *IEEE Trans. Magn*., 42 (2006) No. 8, 1944-1957
[18] Smith R. C., Dapino M.J and Seelecke S., Free Energy Model for Hysteresis in Magnetostrictive Transducers, *Journal of Applied Physics*., 93 (2003), 458–466
[19] Jiles D.C., and Atherton D.L., Theory of Ferromagnetic Hysteresis, *Journal of Magnetism and Magnetic Materials*., 61 (1986), 48-60
[20] Dapino M.J., Smith R.C., Flatau A.B., Structural Magnetic Strain for Magnetostrictive Transducers, *IEEE Trans. Magn.*, 36 (2000), No. 3, 545-556
[21] Perevertov O and Schäfer R., Influence of Applied Compressive Stress on the Hysteresis Curves and Magnetic Domain Structure of Grain-oriented Transverse Fe–3%Si Steel, *Journal of Physics D: Applied Physics*., 45 (2012), 1-10
[22] Rasilo P., Singh D., Belahcen A and Arkkio A., Iron Losses Magneto-elasticity and Magnetostriction in Ferromagnetic Steel Laminations, *IEEE Trans. Magn.*, 49 (2013), 2041 -2044
[23] Zheng J., Cao S., Wang H and Huang W., Hybrid Genetic Algorithms for Parameter Identification of a Hysteresis Model of Magnetostrictive Actuators, *Neurocomputing.*, 70 (2007), 749-761
[24] Liu R and Li L., Simulated Annealing Algorithm Coupled With a Deterministic Method for Parameter Extraction of Energetic Hysteresis Model. *IEEE Trans. Magn.*, 54 (2018), No.11, 1-5
[25] Azoum K., Besbes M., Bouillault F and Ueno, T., Modeling of Magnetostrictive Phenomena. Application in Magnetic Force Control, *The European Physical Journal Applied Physics*, 36 (2006), 43-47
[26] Benbouzid M.E.H., Reyne G and Meunier G., A 2D Dynamic Formulation For Nonlinear Finite Element Modelling of Terfenol-D Rods, *Second International Conference on Computation in Electromagnetics.*, (1994), 52-55
[27] Stachowiak D., Finite Element Analysis of the Active Element Displacement in a Giant Magnetostrictive Transducer, *COMPEL-The International Journal for Computation and Mathematics in Electrical and Electronic Engineering.*, 35 (2016), 1371-1381
[28] Ueno T., Qiu J., and Tani J., Magnetic Force Control Based on the Inverse Magnetostrictive Effect. *IEEE Trans. Magn.,* 40 (2004), No. 3, 1601-1605